

High-sensitivity all-optical PA spectrometer based on fast swept laser interferometry

Xuefeng Mao^{*}, Xiaoyan Ji, Yuting Tan, Hao Ye, Xiaofa Wang

Chongqing University of Posts and Telecommunications, Chongqing 400065, China

ARTICLE INFO

Keywords:

Swept laser interferometry
Fiber-optic acoustic sensor
Photoacoustic spectroscopy
Trace gas detection

ABSTRACT

A high-sensitivity all-optical photoacoustic spectroscopy based on fast swept laser interferometry is proposed to trace gas detection. The momentary cavity length of the fiber-optic Fabry–Perot microphone is demodulated by a fast swept-laser interferometry with an instantaneous frequency demodulation algorithm. The all-optical photoacoustic spectroscopy based on the designed microphone was tested for trace acetylene gas detection in the near-infrared region. The normalized noise equivalent absorption coefficient for acetylene gas is achieved to be $1.06 \times 10^{-9} \text{ cm}^{-1} \text{ W Hz}^{-1/2}$.

1. Introduction

Trace gas detection is crucial in a wide range of applications, such as atmospheric environment [1,2], medical diagnosis [3,4] and industrial processes [5,6]. Photoacoustic spectroscopy (PAS) has easy access to achieve high sensitivity for trace gas detection due to its characteristic of background-free absorption. Typically, photoacoustic (PA) signal is excited by a modulated light source, and is detected by a microphone. The concentration of a gas is proportional to the intensity of the PA signal, so the gas can be quantified by a microphone. The performance of microphone often determines the detection limit of PAS system.

Electric microphones [7,8] and quartz tuning forks [9,10] are often used to measure PA pressure in PAS system. For the past few years, some optical acoustic sensors such as interferometric cantilever [11–13] and fiber-optic microphone [14–16] have been reported for PAS. In interferometric cantilever-based PAS system, the vibration of the micro-mechanical cantilever caused by PA pressure is converted into the phase change of the interference light by Michelson interferometer. However, Michelson interferometer is bulky and hard to calibrate. In addition, the demodulated result is affected by optical path changes derived from temperature variation and vibration. Fiber-optic Fabry–Perot interferometer (FFPI) acoustic sensors, as one of the most reliable and compact optical acoustic sensors, have been used for PA pressure detection. Signal demodulation method is the key technology of FFPI acoustic sensors. Intensity-based quadrature point (Q point) demodulation is a common method for FFPI acoustic sensor, with the advantages of simplicity and high-speed. In our previous work, an

all-optical photoacoustic spectrometer with a polyetherimide diaphragm-based FFPI acoustic sensor as the core has been developed for the detection of trace gases [14]. The detection limit of trace acetylene (C_2H_2) is demonstrated to be 1.3 parts-per-billion (ppb).

In all-optical photoacoustic spectrometer proposed previously by us, the FFPI acoustic sensor employed a probe laser to track the Q point, at which the sensor has maximum sensitivity and dynamic range. However, the Q point easily shifts as a result of environmental fluctuations [17]. If the wavelength of the laser cannot keep track of this point in time, the measured PA signal will be unstable. Spectral demodulation, proved to be a very sensitive method with the capability of absolute measurement, is another method of FFPI acoustic sensors demodulation [18]. It is based on detection of the reflection spectrum of the FFPI acoustic sensor with a white light interferometry (WLI) system. Once the reflection spectrum is obtained, a variety of demodulation methods may be used to recover the absolute cavity length. A conventional WLI system comprises a broadband source and a spectrometer. However, this combination then has low optical power density and wavelength resolution, which will influence the signal-to-noise ratio (SNR) of the system. Furthermore, high-speed spectrometers are expensive and bulky in the near-infrared band in general.

In this paper, a fast swept laser interferometry (FSLI) based fiber-optic PA spectrometer for trace gas detection is presented. The variation of absolute cavity length of the fiber-optic Fabry–Perot microphone caused by photoacoustic signal is demodulated utilizing an interference spectrum, which is captured by a high-speed swept-laser interferometer. An instantaneous frequency demodulation algorithm based on Hilbert

^{*} Corresponding author.

E-mail address: maoxf@cqupt.edu.cn (X. Mao).

<https://doi.org/10.1016/j.pacs.2022.100391>

Received 29 May 2022; Received in revised form 11 August 2022; Accepted 15 August 2022

Available online 19 August 2022

2213-5979/© 2022 The Author(s). Published by Elsevier GmbH. This is an open access article under the CC BY-NC-ND license (<http://creativecommons.org/licenses/by-nc-nd/4.0/>).

transformation that can eliminate the Doppler effect caused by frequency sweep is illustrated. The performance of the proposed all-optical PA spectrometer is demonstrated by trace C_2H_2 detection.

2. Fiber-optic microphone based on FSLI

A highly sensitive fiber-optic microphone has been specially designed for all-optical PA spectrometer. Fig. 1 shows a general configuration of a fiber-optic microphone based on FSLI. It consists of a swept laser, a coupler, an etalon (FSR=50 GHz), a circulator, a sensor head, two photodiodes, high-speed data acquisition card with max sampling rate 80 MHz (PCIe8514, ART Technology), a computer, and optical fibers to connect all the optics. The key parameters of the swept laser are wavelength scanning speed, which determines the upper limit of the frequency of the detected acoustics signal. In this paper, a swept laser is fabricated based on a sampled grating distributed Bragg reflector (SG-DBR, Photonteck) laser diode with a tuning range of 1528–1568 nm, a wavelength tuning speed of up 80,000 nm/s, and a linewidth of less than 5 MHz. The wavelength information can be acquired simultaneously through a wavelength calibration channel by the etalon. The sampling of the spectrum and the wavelength is synchronously triggered by an external square wave signal of a laser controller. The sensor head of the FFPI acoustic sensor whose Fabry–Perot cavity is formed by the fiber end face and the diaphragm is made up of a silica tube, a silica ferrule, and a polyethylene terephthalate (PET) film. The detailed description of the sensor head can be found in reference [19].

Theoretically, as long as the frequency of the laser scanning entire spectrum is greater than twice the frequency of the PA signal, this signal can be restored. Many WLI demodulation algorithms have been developed for spectral demodulation. Unfortunately, it is not suitable for WLI system based on swept-lasers. In the process of spectrum acquisition, Doppler phenomena will give birth to the interference spectrum and lead to the demodulation error [20]. To overcome the Doppler induced demodulation error, an instantaneous frequency (IF) demodulation algorithm is proposed for the single frequency PA signal collected by the all-optical PA spectrometer. The interference spectrum of a low-finesse FFPI sensor can be expressed as

$$I(\nu) = I_0 \left[1 + \gamma \cos \left(\frac{4\pi n L}{c} \nu + \varphi_0 \right) \right] \quad (1)$$

where I_0 is the output intensity of the laser source, γ is the fringe visibility of the FFPI sensor, n is the refractive index of the cavity, L is the cavity length, c is the speed of light in vacuum, ν is the frequency of the laser, φ_0 is the initial phase. Then, after filtering out the DC component and normalization, (1) can be rewritten as

$$I(\nu) = \cos \left(\frac{4\pi n L}{c} \nu + \varphi_0 \right) \quad (2)$$

Hilbert transformation of Eq. (2) can be expressed as

$$H[I(\nu)] = \sin \left(\frac{4\pi n L}{c} \nu + \varphi_0 \right) \quad (3)$$

where H is the Hilbert transform. According to Eqs. 2 and 3, the total phase Φ of the interference spectrum can be expressed as

$$\Phi = \frac{4\pi n L}{c} \nu + \varphi_0 = \arctan \left(\frac{H[I(\nu)]}{I(\nu)} \right) \quad (4)$$

Therefore, the transient cavity length L can be obtained by taking any two frequency values and substituting them into Eq. 4. Then, the absolute value of instantaneous cavity length can be expressed as

$$L = \frac{\arctan(H[I(\nu_2)]/I(\nu_2)) - \arctan(H[I(\nu_1)]/I(\nu_1))}{\nu_2 - \nu_1} \cdot \frac{c}{4\pi n} \quad (5)$$

The limit sensitivity of a PAS spectrometer is influenced by the length resolution of the cavity. So, the cavity length resolution of the acoustic sensor is tested first. No acoustic pressure acted on the FFPI sensor, which means the cavity length was fixed. The interference spectrum measured by the FSLI system is shown in Fig. 2 and the SNR is calculated to be 34.2 dB. To shorten the time of one round-trip scanning, the scanning range of 5 nm (1545–1550 nm) is actually used, as shown in the illustration of Fig. 2. At 5-nm-range full speed scan, more than 16k data points were recorded in barely more than 1 s. The absolute cavity length was calculated to be 1305 μm by the high-speed demodulation algorithm. The standard deviation of the entire data set was calculated to be 66 pm. The high resolution derives from the high SNR of the

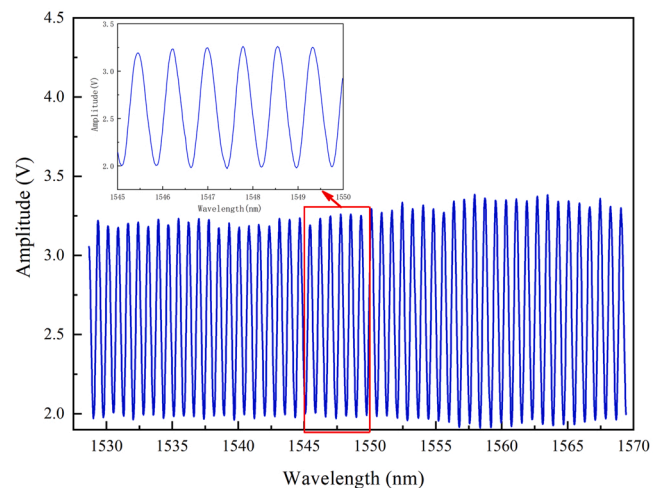


Fig. 2. Interference spectrum of the designed fiber-optic microphone.

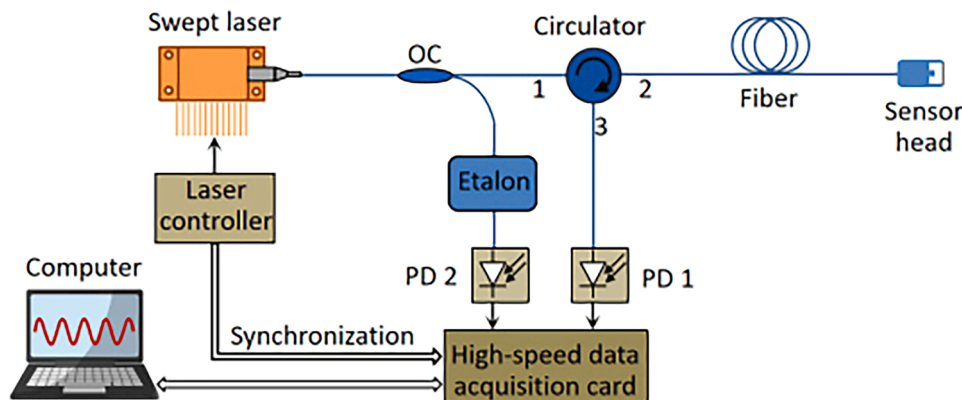


Fig. 1. Schematic diagram of a fiber-optic microphone based on fast swept laser interferometry.

interference spectrum caused by the laser's high power and narrow linewidth. The first 1k demodulated OPD data points and the frequency count of the data are shown in Fig. 3.

As sine wave acoustic signals were applied to the head sensor, modulations were observed on the demodulated OPD of the FFPI cavity. The time domain responses of the FFPI acoustic sensor were tested when the acoustic pressure and frequency were set to be 25 mPa and 1 kHz, 2 kHz, 4 kHz, respectively. The first 100 data points of the demodulated OPD recorded in the 1 kHz, 2 kHz and 4 kHz tests are shown in Fig. 4. It is worth noting that every point in these data sets actually represents an independent absolute measurement of deviation from the static cavity length. The demodulated static cavity length as a function of temperature is plotted in Fig. 5. Owe to the IF demodulation method, the cavity length demodulation is free from temperature variation.

To compare the performance of the proposed IF demodulation and the quadrature demodulation, a comparison experiment was carried out. The two demodulation schemes shared the experimental apparatus and faced the same acoustic pressure. In the quadrature demodulation, the Q point was locked by tuning wavelength to obtain high sensitivity. When an acoustic pressure of 20 mPa is applied at 1 kHz, the spectrogram of the acoustic pressure signals was recorded by two methods of demodulation respectively, as shown in Fig. 6 (Ref. 20 μ Pa). The noise floors are about 17.81 and 4.9 dB respectively for the same FFPI sensor with 1 Hz resolution bandwidth. This implies that the SNR of the IF demodulation is over 3 times higher than the quadrature demodulation.

3. Experimental system and results

The schematic diagram of the experimental system based on PAS is shown in Fig. 7. It consists of a NIR tunable fiber laser (NIR-TFL), an erbium-doped fiber amplifier (EDFA), an optical fiber collimator, a first-order longitudinal resonant PA cell, a PA demodulator and a computer. The NIR-TLS has built-in wavelength modulation and scanning functions, and the real-time wavelength of the laser can be transmitted to the computer. The detailed description of the NIR-TLS can be got in Ref. [14]. The high-power laser light is collimated into the first-order longitudinal resonant PA cell, which is composed of a cylindrical acoustic resonant tube, two buffer volumes, and a gold coated mirror. The length and the inner diameter of the brass resonant tube are 120 mm and 8 mm, respectively. In addition, the quality factor of the PA cell is calculated to be 28.2. The acquired interference spectrum containing second-harmonic PA signal is first processed by the IF demodulation algorithm with high sensitivity. Then the demodulated dynamic cavity length of the fiber-optic Fabry-Perot microphone is input to a virtual lock-in amplifier implemented by LabView, which can promote the SNR.

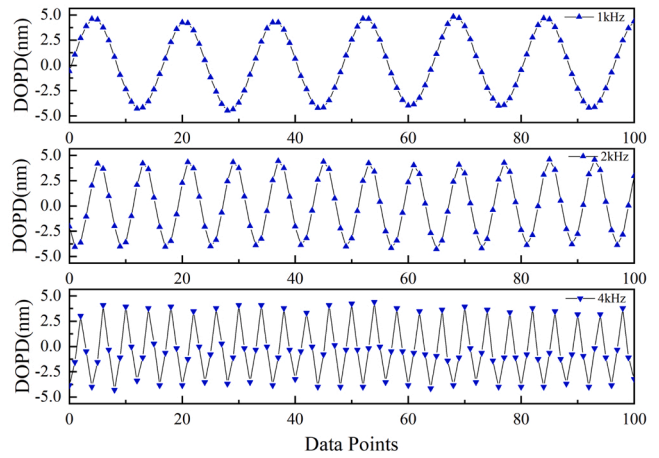


Fig. 4. First 100 data points of the demodulated OPD in 1 kHz, 2 kHz and 4 kHz tests.

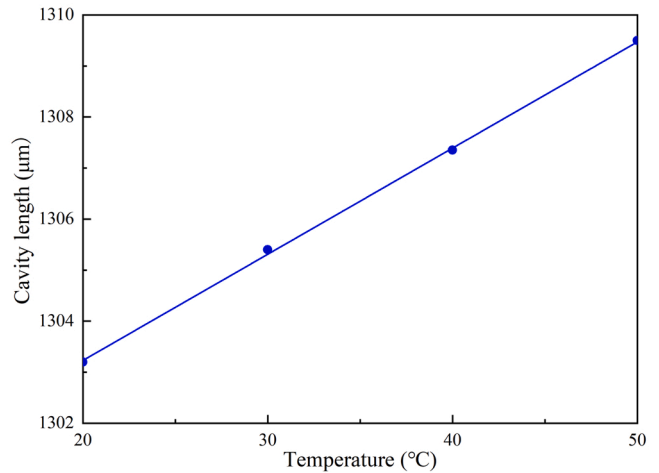


Fig. 5. Static cavity length as a function of temperature.

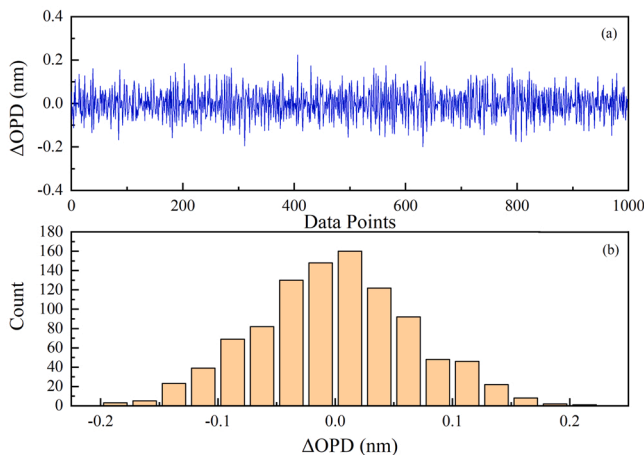


Fig. 3. (a) First 1k data points of the demodulated OPD change in the fixed cavity length test. (b) Frequency count of the data shown in (a).

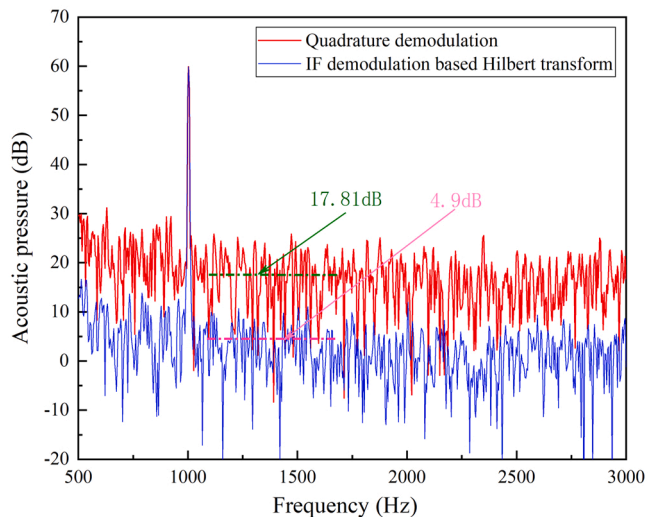


Fig. 6. Spectrogram of 20 mPa acoustic pressure with the IF demodulation based on Hilbert transform and quadrature demodulation respectively at 1 kHz.

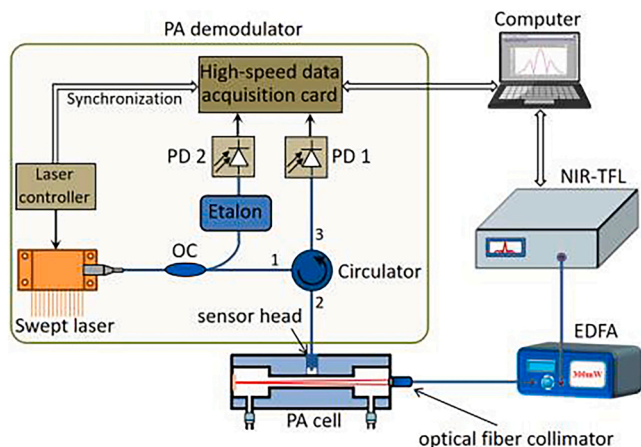


Fig. 7. Schematic diagram of the PA system for trace C₂H₂ detection.

The acoustic resonance frequency of the first-order resonant PA cell was measured experimentally. The C₂H₂ with the concentration of 100 ppm was filled into the PA cell, and the modulation frequencies were scanned from 500 Hz to 800 Hz with the wavelength of the laser light is locked to 1531.59 nm at 30 °C. With the second-harmonic wavelength modulation spectroscopy (2 f-WMS) technique, the frequency response of the PA system is shown in Fig. 8. The resonant frequency peak can be obtained to be 1332 Hz. As a consequence, the frequency of the sinusoidal modulation signal is set to be 666 Hz. As mentioned earlier, the laser scan frequency in the PA demodulator is 16 kHz which is much higher than the frequency of the 2f PA signal.

To test the performance of the FSLI-based fiber-optic PA spectrometer, C₂H₂ gas with different concentrations were filled into the PA cell successively. The gas mixing system was made up of a 1 ppm C₂H₂/N₂ gas mixture, a pure N₂ gas, and two mass flow controllers (MFCs) with an error of ±0.2 % (LF420-S and LF485-S, LF Technology). Various C₂H₂ concentrations gas can be obtained by controlling the volume ratios of the two gases, and then flowed into the PA cell. The integration time of the virtual lock-in amplifier was set to be 100 ms. The Fig. 9 shows the denoised 2f-WMS signals for seven different C₂H₂ concentration levels of 1, 5, 10, 25, 50, 75 and 100 ppm, respectively. The linearity response of the FSLI-based fiber-optic PA spectrometer is checked, and the result is shown in Fig. 10. The linear fitting R² is 0.996, which proves that the PAS system has a good linear response at C₂H₂ concentration from 0 to 100 ppm. The responsivity of the proposed PA system is estimated to be

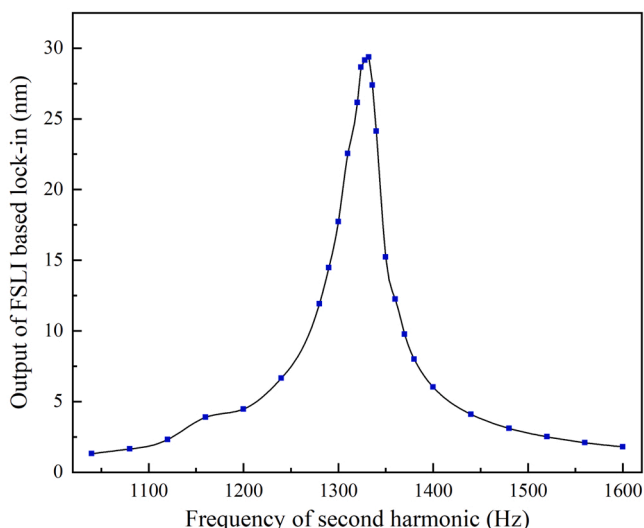


Fig. 8. Experimental frequency responses of the PA system.

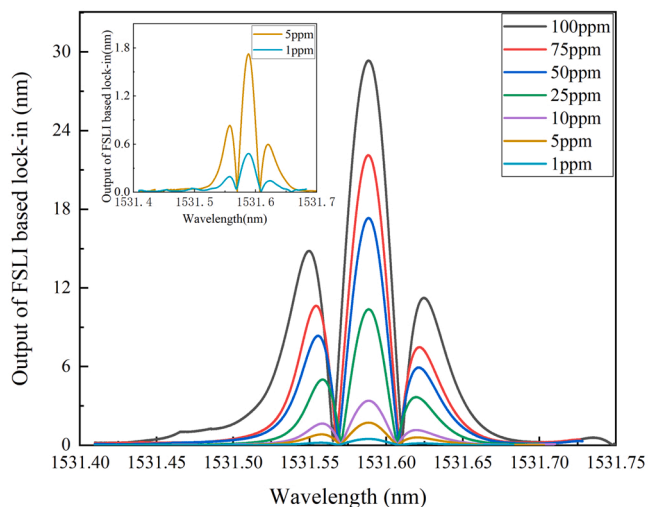


Fig. 9. 2f-WMS signals with different concentrations of C₂H₂/N₂ gas mixture.

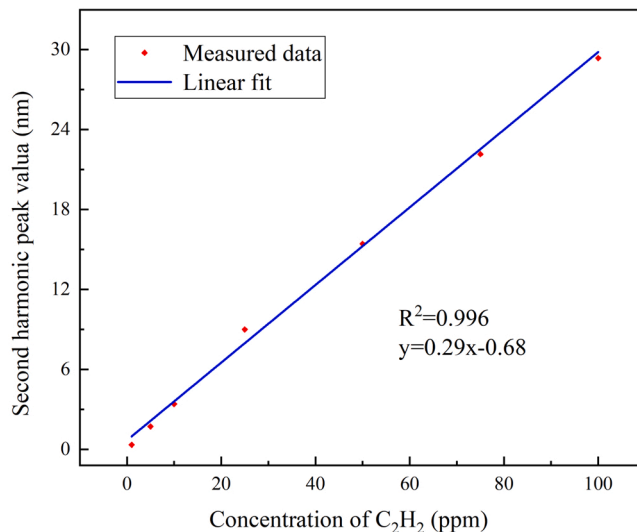


Fig. 10. The PA signals as a function of C₂H₂ concentrations.

0.29 nm/ppm by linear fitting at C₂H₂ detection.

To further evaluate the performance of the FSLI-based fiber-optic PA spectrometer, an Allan deviation analysis was performed to investigate the limit of detection (LOD) and the stability. The background noise was measured by the PA cell filled with pure N₂ gas. The output of the PA system is checked by the 2 f-WMS technique with the excitation light source turned on, during the measurement process. The inset of the Fig. 11 shows the background noise over 2000 s when the integration time of the lock-in amplifier was 10 s. The standard deviation of noise is estimated to be 0.19 pm. According to the responsivity of 0.29 nm/ppm, the LOD can be calculated to be 0.66 ppb. The normalized noise equivalent absorption (NNEA) coefficient can be calculated to be $1.06 \times 10^{-9} \text{ cm}^{-1} \text{ W Hz}^{-1/2}$. Fig. 11 shows the Allan deviation as a function of the averaging time τ . It indicates that the Allan deviation decreases as the averaging time decreases in the range less than 700 s, which proves that the designed PA spectrometer is stable during the test time. From Fig. 11, the Allan deviation is 0.013 pm with an averaging time of 300 s. The corresponding estimated MDL is 45 ppt.

4. Conclusion

A fast swept-laser interferometry (FSLI) based fiber-optic PA

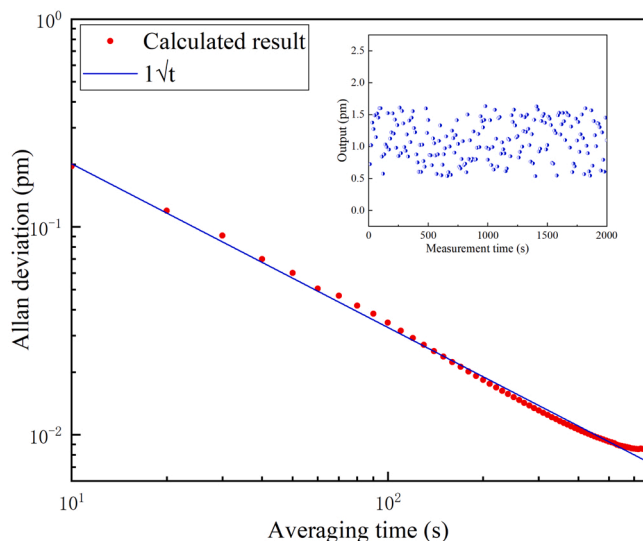


Fig. 11. Allan deviation as a function of the data averaging period. Inset: The measured background noise by filling the PA cell with pure N_2 .

spectrometer is developed and experimentally demonstrated for trace acetylene gas detection, with advantages of high sensitivity and high stability. The cavity length of the fiber-optic Fabry–Perot microphone is demodulated by a fast swept-laser interferometry with an instantaneous frequency demodulation algorithm. Real-time cavity length demodulation is successfully demonstrated by utilizing the instantaneous frequency demodulation, which contributes to immune from the fluctuation of the light source power and optical loss. Experimental result verifies that the SNR of the instantaneous frequency demodulation is over 3 times higher than the quadrature demodulation. Trace C_2H_2 gases of different concentrations were measured using the laser wavelength of 1531.59 nm by the 2f-WMS detection method. Experimental results show that the demodulated PA signal has an excellent linear response to the concentration. The NNEA coefficient of C_2H_2 is achieved to be $1.06 \times 10^{-9} \text{ cm}^{-1} \text{ W Hz}^{-1/2}$. Furthermore, by using Allan variance analysis, the LOD is estimated to be 45 ppt for an integration time of 300 s

Funding

China Postdoctoral Science Foundation Funded Project (No.:2018M633315).

Declaration of Competing Interest

The authors declared that they have no conflicts of interest to this work.

Data availability

Data will be made available on request.

References

- [1] Jinbao Xia, et al., A ppb level sensitive sensor for atmospheric methane detection, *Infrared Phys. Techn.* 86 (2017) 194–201.
- [2] Y. Cao, N.P. Sanchez, W. Jiang, R.J. Griffin, F. Xie, L.C. Hughes, F.K. Tittel, Simultaneous atmospheric nitrous oxide, methane and water vapor detection with a single continuous wave quantum cascade laser, *Opt. Express* 23 (3) (2015) 2121–2132.
- [3] J.A. Covington, et al., The application of FAIMS gas analysis in medical diagnostics, *Analyst* 140 (20) (2015) 6775–6781.
- [4] Valentine Saasa, et al., Sensing technologies for detection of acetone in human breath for diabetes diagnosis and monitoring, *Diagnostics* 8.1 (2018) 12.
- [5] Chengwei Wen, Xin Huang, Chunlei Shen, Multiple-pass enhanced Raman spectroscopy for fast industrial trace gas detection and process control, *J. Raman Spectrosc.* 51.5 (2020) 781–787.
- [6] Lei Shu, Mithun Mukherjee, Xiaoling Wu, Toxic gas boundary area detection in large-scale petrochemical plants with industrial wireless sensor networks, *IEEE Commun. Mag.* 54.10 (2016) 22–28.
- [7] Zhenfeng Gong, et al., Photoacoustic spectroscopy based multi-gas detection using high-sensitivity fiber-optic low-frequency acoustic sensor, *Sens. Actuat. B-Chem.* 260 (2018) 357–363.
- [8] M.J. Navas, A.M. Jiménez, A.G. Asuero, Human biomarkers in breath by photoacoustic spectroscopy, *Clin. Chim. Acta* 15-16 (2012) 1171–1178.
- [9] Y. Ma, Y. He, L. Zhang, et al., Ultra-high sensitive acetylene detection using quartz-enhanced photoacoustic spectroscopy with a fiber amplified diode laser and a 30.72 kHz quartz tuning fork, *Appl. Phys. Lett.* 110 (3) (2017), 031107.
- [10] H. Wu, L. Dong, H. Zheng, et al., Beat frequency quartz-enhanced photoacoustic spectroscopy for fast and calibration-free continuous trace-gas monitoring, *Nat. Commun.* (2017) 8.
- [11] V. Koskinen, et al., Progress in cantilever enhanced photoacoustic spectroscopy, *Vib. Spectrosc.* 48.1 (2008) 16–21.
- [12] Teemu Tomberg, et al., Cavity-enhanced cantilever-enhanced photo-acoustic spectroscopy, *Anal* 144.7 (2019) 2291–2296.
- [13] Jari Peltola, et al., High sensitivity trace gas detection by cantilever-enhanced photoacoustic spectroscopy using a mid-infrared continuous-wave optical parametric oscillator, *Opt. Express* 21.8 (2013) 10240–10250.
- [14] X. Mao, X. Zhou, Z. Gong, et al., An all-optical photoacoustic spectrometer for multi-gas analysis, *Sens. Actuators B Chem.* 232 (2016) 251–256.
- [15] Zhenfeng Gong, et al., Ppb-level detection of methane based on an optimized T-type photoacoustic cell and a NIR diode laser, *Photoacoustics* 21 (2021), 100216.
- [16] Y. Tan, C. Zhang, W. Jin, et al., Optical fiber photoacoustic gas sensor with graphene nano-mechanical resonator as the acoustic detector, *IEEE J. Sel. Top. Quantum Electron.* 23 (2) (2017) 1–11.
- [17] Yupeng Zhu, Ming Han, Passive quadrature demodulation of birefringent low-finesse fiber-optic Fabry–Perot interferometric sensors, *Opt. Lett.* 45.13 (2020) 3419–3422.
- [18] Cheng Ma, Anbo Wang, Signal processing of white-light interferometric low-finesse fiber-optic Fabry–Perot sensors, *Appl. Opt.* 52.2 (2013) 127–138.
- [19] X. Mao, et al., Stabilized fiber-optic Fabry–Perot acoustic sensor based on improved wavelength tuning technique, *J. Light. Technol.* 35.11 (2017) 2311–2314.
- [20] Erik A. Moro, D.Todd Michael, D.Puckett Anthony, Understanding the effects of Doppler phenomena in white light Fabry–Perot interferometers for simultaneous position and velocity measurement, *Appl. Opt.* 51 (27) (2012) 6518–6527.



Xuefeng Mao received the Ph.D. degree from the School of Physics and Optoelectronic Technology, Dalian University of Technology, Dalian, China, in 2016. He is currently an associate professor in the College of optoelectronic engineering, Chongqing University of Posts and Telecommunications, Chongqing, China. His research interests include environmental sensing technology and fiber-optic sensors.